Chinese Physics Letters

LETTER

Universal Scaling of Higher-Order Cumulants in Quantum Isotropic Spin Chains

Cite as: Shixian Jiang *et al*. 2026 *Chin. Phys. Lett.* **43** 070302

Recommended Articles

Complete Universal Scaling in First-Order Phase Transitions
Fan Zhong
Chin. Phys. Lett. **41**, 100502 (2024)

Complete Universal Scaling of First-Order Phase Transitions in the Two-Dimensional Ising Model
Yuxiang Zhang, and Fan Zhong
Chin. Phys. Lett. **42**, 090001 (2025)

Uncovering Hidden Spin of Scalar Fields with Higher-Order Derivative Lagrangian: On the Wave Spin in Drifted and Dissipative Fields
Shuo Xin, Mengxiang Xie, and Jie Ren
Chin. Phys. Lett. **42**, 064301 (2025)

Thermal Entanglement in Disordered Spin Chains: Localization, Thresholds, and the Quantum-to-Classical Crossover
Dihang Sun, Zhigang Hu, and Biao Wu
Chin. Phys. Lett. **42**, 070601 (2025)

Universal Scaling Laws in Quantum-Probabilistic Machine Learning by Tensor Network: Toward Interpreting Representation and Generalization Powers
Sheng-Chen Bai, and Shi-Ju Ran
Chin. Phys. Lett. **41**, 120701 (2024)

Higher-Order Topological States in Chiral Split Magnons of Honeycomb Altermagnets
Xuan Guo, Meng-Han Zhang, and Dao-Xin Yao
Chin. Phys. Lett. **42**, 120703 (2025)

A series journal of Chinese Physical Society distributed by IOP Publishing

Chinese Physics Letters

Chin. Phys. Lett. **43** 070302 (2026)

LETTER

DOI: 10.1088/0256-307X/43/7/070302
CSTR: 32039.14.0256-307X.43.7.070302

Universal Scaling of Higher-Order Cumulants in Quantum Isotropic Spin Chains

Shixian Jiang(蒋仕贤)[1,†], Jianpeng Liu(刘建鹏)[1,2,3,†], Jianmin Yuan(袁建民)[4,1], Xi-Wen Guan(管习文)[5,6,7], and Yongqiang Li(李永强)[1,2,3,*]

[1]College of Science, National University of Defense Technology, Changsha 410073, China
[2]Hunan Key Laboratory of Extreme Matter and Applications, National University of Defense Technology, Changsha 410073, China
[3]Hunan Research Center of the Basic Discipline for Physical States, National University of Defense Technology, Changsha 410073, China
[4]Institute of Atomic and Molecular Physics, Jilin University, Changchun 130012, China
[5]Innovation Academy for Precision Measurement Science and Technology, Chinese Academy of Sciences, Wuhan 430071, China
[6]NSFC-SPTP Peng Huanwu Center for Fundamental Theory, Xi'an 710127, China
[7]Department of Fundamental and Theoretical Physics, Research School of Physics, Australian National University, Canberra ACT 0200, Australia

[†]These authors contributed equally to this work
[*]Corresponding author. Email: li_yq@nudt.edu.cn

Understanding universal behavior of far-from-equilibrium transport dynamics at a quantum many-body level is a longstanding challenge. A full characterization of universal dynamics of nonlocal correlation functions still remains largely unknown. In this letter, we uncover universal scaling laws of higher-order cumulants in one-dimensional isotropic Heisenberg model, revealing anomalous behaviors of nonequilibrium dynamics exclusively accessible in higher-order correlation functions. Using numerical simulations and full counting statistics, we determine the power laws of both the spin polarization transfer and contrast cumulants for different kinds of helix and domain-wall initial states. Building on such physical states, we unify the scaling behavior of the higher-order cumulants as two types of dynamics: anomalous diffusive and superdiffusive. For the former, these higher cumulants show a deviation from Gaussian statistics, with the scaling exponents being identical for the first four orders. For the latter, however, we observe a breakdown of KPZ universality, with the exponents of the third and fourth orders differing significantly from those of the first two. Our results are also agreeable with recent experimental observations, advancing understanding of far-from-equilibrium transport phenomena.

Introduction

Characterization of quantum transport in many-body systems with charge fluctuations, spin currents, etc., is truly one of the frontiers in physics [1−6]. It has been understood in general that conserved quantities present universal scaling-invariant macroscopic transport, including ballistic, superdiffusive and diffusive propagation, regardless of microscopic scenarios [7−18]. Such emergent many-body hydrodynamics has been widely predicted in quantum systems, even in conditions far from equilibrium, high temperature, or disordered, deepening our understanding of quantum dynamical criticality [19−27]. However, a comprehensive classification of nonequilibrium dynamics necessitates going beyond the local observations, as higher-order correlations commonly reveal distinct scaling behavior.

Higher-order cumulants serve as a vital tool for probing multipoint correlations and revealing fundamental insights into non-Gaussian transport [28,29]. It is generally accepted that ballistic transport universally exhibits linear temporal scaling for all cumulant orders [30,31], whereas diffusive transport manifests order-dependent scaling whose general form remains unresolved [32]. As promising platforms for the investigation of far-from-equilibrium dynamics, the quantum simulations and quantum circuits drastically leverage single-site addressing to probe multipoint correlations. Recent experimental breakthroughs have been achieved for the study of elusive higher-order cumulants in far-from-equilibrium dynamics: e.g., in the chaotic systems, generic initial states exhibit identical diffusive scaling in both first- (density) and second-order cumulants (density fluctuations) [33]. For the integrable isotropic Heisenberg spin chain, state-dependent transport behavior is observed in the first-order cumulant, i.e., the Kardar–Parisi–Zhang (KPZ) superdiffusion emerges for the domain-wall (DW) initial state [34], in contrast to the diffusive transport for spin-helix (SH) initial state [35−37]. It was also evidenced for the DW initial state that higher-order cumulants deviate from KPZ superdiffusive dynamics [38,39]. However, this observation of the dynamical universality for the DW state remains in debate [32,40,41]. Meanwhile, scaling behavior of the higher-order cumulants for the SH state is still an open problem.

In this Letter, we uncover such miscellaneous scaling behavior of higher-order cumulants for different experimentally realizable initial states in the one-dimensional (1D) isotropic Heisenberg chain, typically the SH [35−37] and DW states [34,38]. Using time-dependent variational principle (TDVP) algorithm and full counting statistics (FCS) [32,39,42−47], we perform large-scale calculations on the higher-order cumulants, revealing two distinct types of anomalous quantum transport in experimentally accessible timescales. For the SH initial state, the non-Gaussian statistics appear in the third- and fourth-order cumulants and they share the same scaling exponents with the first two. Whereas for the DW initial state, the third and fourth orders exhibit distinct temporal exponents from the first two, with the standardized cumulant deviating from the KPZ conjecture. We demonstrate that the instability in the fourth-order cumulant is attributed to genuine long-time fluctuations at many-body level. To solidify this framework, we further study the higher-order cumulants for a multi-periodic domain-wall (MPDW) state with specific local spin polarization patterns. Our results confirm the recent experimental observations of the first few cumulants [34,35,38] and open a promising way to identify universal temporal scaling exponents for different initial states in different quantum systems in current experiments.

Model and Methods

We study the isotropic 1D Heisenberg spin chain, whose

Received 3 April 2026; accepted 9 June 2026; published 7 July 2026
© 2026 Chinese Physical Society and IOP Publishing Ltd. All rights, including for text and data mining, AI training, and similar technologies, are reserved.

Check for updates

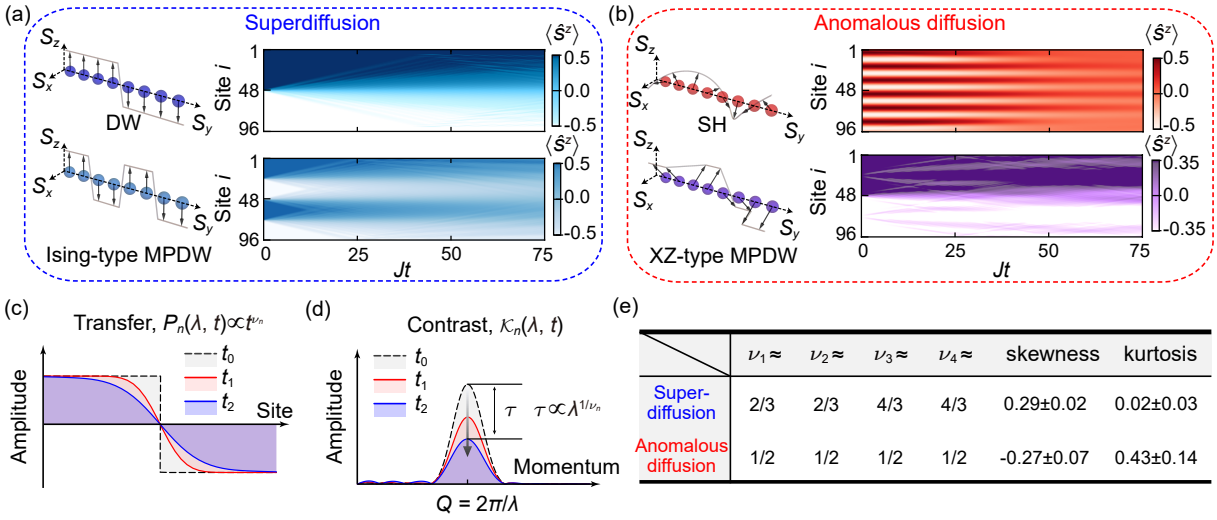

	$\nu_1\approx$	$\nu_2\approx$	$\nu_3\approx$	$\nu_4\approx$	skewness	kurtosis
Super-diffusion	2/3	2/3	4/3	4/3	0.29±0.02	0.02±0.03
Anomalous diffusion	1/2	1/2	1/2	1/2	-0.27±0.07	0.43±0.14

Fig. 1. Cumulant scaling and its exponents in the isotropic Heisenberg spin chain. Far-from-equilibrium dynamics of spin polarization $\langle\hat{S}_i^z\rangle$ for initial states: (a) DW [34,38] and Ising-type MPDW states, and (b) SH [35,37] and XZ-type MPDW states, which respectively show superdiffusive and anomalous diffusive dynamics. The contour plots illustrate the time evolution of initial real-space spin distributions. The nth-order cumulants are illustrated at different time ($t_0 < t_1 < t_2$): (c) the spin polarization transfer across the domain wall and (d) the contrast for a wavevector $Q = 2\pi/\lambda$, where ν_n denotes the scaling exponent of nth-order cumulant. (e) shows table of the scaling exponents of first four orders $\nu_{1,2,3,4}$ and standardized cumulants of the third (skewness) and fourth orders (excess kurtosis) with errors for these two types of distinct long-time dynamics obtained by (c) and (d).

Hamiltonian reads

$$\hat{H} = -J\sum_i(\hat{S}_i^x\hat{S}_{i+1}^x + \hat{S}_i^y\hat{S}_{i+1}^y + \hat{S}_i^z\hat{S}_{i+1}^z), \tag{1}$$

where $\hat{S}_i^{x,y,z}$ denotes the spin-1/2 operators at site i, and $J = 1$ is the coupling strength, and open boundary conditions are used throughout this work. The Hamiltonian of Eq. (1) possesses a global SU(2) symmetry, conserving all total spin components and determining macroscopic transport in the long-time scale [48]. The experimentally relevant DW and SH initial states are respectively written as $|\varphi_{\rm DW}\rangle = |\uparrow\rangle^{\otimes L/2}\otimes|\downarrow\rangle^{\otimes L/2}$ and $|\varphi_{\rm SH}\rangle = \otimes_i[\cos((Qi+\theta)/2)|\uparrow\rangle_i - \sin((Qi+\theta)/2)|\downarrow\rangle_i]$ with wavevector $Q = 2\pi/\lambda$. λ denotes the wavelength of the initial spin configuration and θ is the initial phase. Two types of distinct quantum transport behavior are observed in local quantities, i.e. for the pure DW state, magnetization transfer exhibits the anomalous scaling of superdiffusion [Figs. 1(a) and 1(c)] [34,38], though ultimately recovering diffusion at late times [49–52]; for the SH state [53], diffusive transport manifested in magnetization contrast emerges within experimentally accessible timescales [Figs. 1(b) and 1(d)] [35,37]. Using the generalized initial MPDW state [Figs. 1(a) and 1(b)], we further establish a unified description of the nonequilibrium transport dynamics [Figs. 1(c) and 1(d)]. The difference between two types of Ising- and XZ-type MPDW state is the local spin-component structure of the initial state. The former has only S_z components and therefore preserves superdiffusion of DW state. The latter shares the same chirality in x-z plane and one may expect the same emergent scaling behavior as SH state [54]. The MPDW states and further details of the initial-state construction are provided in the Supplemental Material (SM).

To characterize higher-order fluctuations in the far-from-equilibrium transport dynamics, we evaluate nth-order cumulants at time t via spin polarization transfer [55–56]

$$\mathcal{P}_n(\lambda,t) = \sum_{i_1,\ldots,i_n}\langle\hat{S}_{i_1}^z\hat{S}_{i_2}^z\ldots\hat{S}_{i_n}^z\rangle_c, \tag{2}$$

with $\hat{S}_i^z \equiv \mathrm{sgn}[\langle\hat{S}_i^z(0)\rangle]\hat{S}_i^z(t)$, where the sgn function fixes the transferred spin polarization based on initial orientation and further forbids cancellations between initially opposite domains. The weighted contrast is obtained by performing Fourier transform at wavevector Q

$$\mathcal{K}_n(\lambda,t) = \sum_{i_1,\ldots,i_n}\langle\hat{Q}_{i_1}^z\hat{Q}_{i_2}^z\ldots\hat{Q}_{i_n}^z\rangle_c, \tag{3}$$

where $\hat{Q}_i^z \equiv -\cos(Qi+\theta)\hat{S}_i^z(t)$, and $\langle\cdots\rangle_c$ denotes the nth-order cumulants composed of n-point operators of $\hat{S}_i^z$ or $\hat{Q}_i^z$ [41,57–59]. In the long-time limit, cumulants are expected to grow asymptotically as $|\Delta\mathcal{P}_n(\lambda,t)| \equiv |\mathcal{P}_n(\lambda,t) - \mathcal{P}_n(\lambda,0)| \propto t^{\nu_n}$ [48], where ν_n is the scaling exponent for the nth order [Figs. 1(c) and 1(e)]. The threshold time τ, extracted from $\mathcal{K}_n(\lambda,t)$ either when it decays to 0.4 ($n = 1$ for local quantities) or reaches its peak position ($n = 2$, 3, or 4 for nonlocal quantities), obeys the scaling law of $\tau\propto\lambda^{1/\nu_n}$ for different λ [Figs. 1(d) and 1(e)]. Specifically, the characteristic length scale associated with the nth-order cumulant grows as $l_n \sim \tau^{\nu_n}$. Then the relaxation or correlation-building time is determined by the condition $l_n \sim \lambda$, which finally gives $\tau\propto\lambda^{1/\nu_n}$. This length–time scaling picture has been widely used to identify transport universality classes [33–35,53]. Note that it remains finite in the thermodynamic limit for fixed λ, but diverges in the long-wavelength limit. To transform dissimilar features into the same scale [38], we introduce standardized cumulants, including skewness $\gamma_3(\lambda,t)$ and excess kurtosis $\gamma_4(\lambda,t)$ [34]. Note here that the first four cumulants represent the mean, variance, asymmetry, and peakedness of statistical distributions, respectively [55].

In order to obtain scaling exponents of the cumulants in the long-time dynamics, we employ TDVP method in terms of the matrix product state framework and the ITensor library [60–62]. Specifically, for the balance of finite-size effects and computational cost, the hybrid two-site and one-site TDVP method is applied [62–64]. To further validate our approach, we also present higher-order cumulants using both FCS and subsystem spin fluctuations. Numerical details and convergence tests are presented in the SM.

First-Order Cumulant via Unified Description

We first analyze the first-order cumulant in far-from-equilibrium transport dynamics of the quantum isotropic Heisenberg chain. Three initial states, including DW, MPDW, and SH states, are investigated to extract scaling behavior in the spin transport. The many-body dynamics is quantified through spin polarization transfer $|\Delta\mathcal{P}_1(\lambda,t)|$ and contrast decay $\mathcal{K}_1(\lambda,t)$ in the experimentally accessible timescales with $Jt \approx 100$.

As expected, for the DW initial state, the transport dynamics exhibits superdiffusive behavior. Figure 2(a) shows the first-order spin polarization transfer for Ising-type MPDW states with wavelengths $\lambda = 24, 32, 48, 96$, where the case $\lambda = L = 96$ corresponds to the single-periodic DW state. Note that dashed lines are guided to clearly

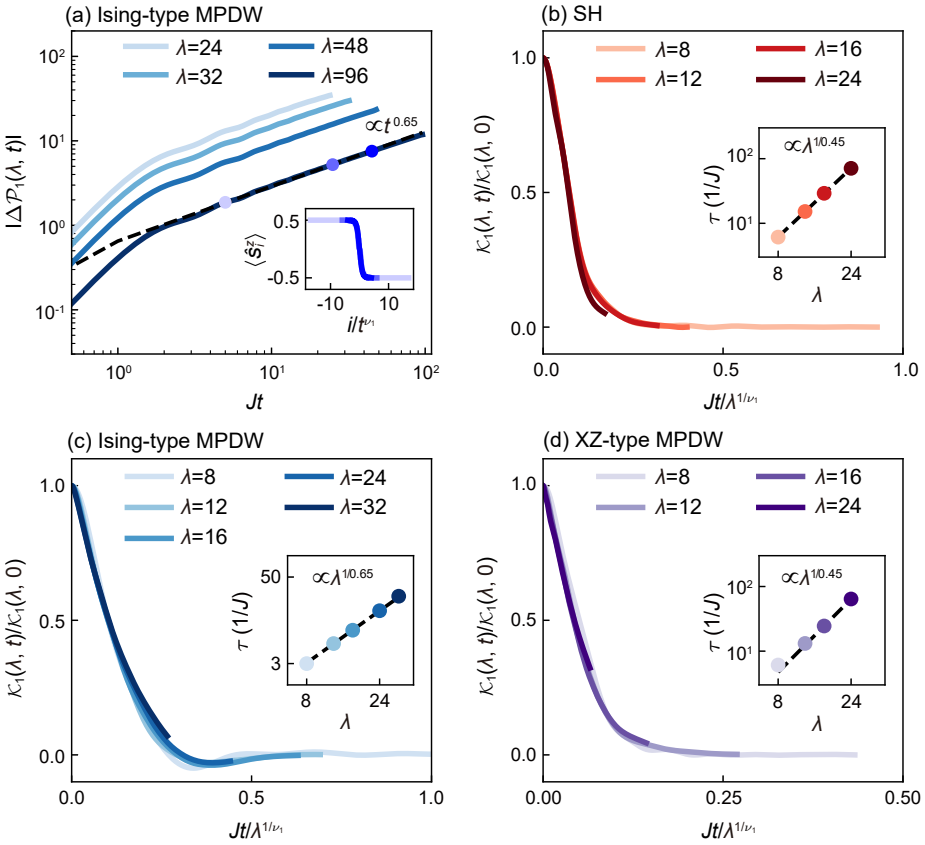

Fig. 2. First-order cumulant of the isotropic Heisenberg chain. (a) shows spin polarization transfer $|\Delta\mathcal{P}_1(\lambda,t)|$ for Ising-type (superdiffusive) initial states with wavelength $\lambda = 24$ to 96. The inset shows rescaled spin distributions for $\lambda = 96$ at time $Jt = 5$, 25, and 45. (b)–(d) Rescaled contrast curve $\mathcal{K}_1(\lambda,t)$ for (b) SH (diffusive), (c) Ising-type MPDW (superdiffusive), and (d) XZ-type MPDW (diffusive) initial states. The insets show the relaxation time τ following a power-law scaling $\tau \propto \lambda^{1/\nu_1}$. For the Ising-type MPDW state, $\nu_1 = 0.65 \pm 0.02$ in (a) is estimated by the sliding-window fitting procedure and $\nu_1 = 0.64 \pm 0.01$ in (c) is estimated by the multi-threshold averaging procedure, which yield consistent superdiffusive dynamics. While diffusive dynamics emerges for the SH state $\nu_1 = 0.45 \pm 0.01$ in (b) and XZ-type MPDW state $\nu_1 = 0.48 \pm 0.01$ in (d), estimated by multi-threshold averaging procedure. See details in the SM. Lattice size is $L = 96$.

illustrate the distinct scaling behavior in this work. The long-time dynamics of the spin polarization transfer exhibits a temporal power-law growth, i.e., $|\Delta\mathcal{P}_1(\lambda,t)| \propto t^{\nu_1}$ with the scaling exponent $\nu_1 \approx 0.65$, confirming prior numerical results [49–52] and experimental observations [34] for the DW initial state. The data collapse of the real-space spin distributions shows a consistency of the rescaling with $\nu_1 = 0.65$ [inset of Fig. 2(a)]. In contrast, for the SH initial state, we observe that a diffusive transport emerges in the long-time dynamics, see the scaling collapse of contrast decay $\mathcal{K}_1(\lambda,t)$ in Fig. 2(b) and the power-law scaling of relaxation time $\tau \propto \lambda^{1/\nu_1}$ in the inset of Fig. 2(b), and also see discussions in [54,65–72]. We note that the resulting exponent $\nu_1 \approx 0.45$ for the SH initial state agrees with the experimental observations [35]. Nevertheless the boundary effects do disrupt the scaling behavior in a finite system. Here we find that a lattice size at least $L = 96$ is necessary to meet our study, see the SM.

In order to provide a unified description for experimentally relevant transport dynamics, we further consider the MPDW initial states to reproduce transport scaling behavior in the isotropic Heisenberg chain. For a Ising-type MPDW initial state, i.e. multi-periodic DW state [Fig. 1(a)], we obtain the superdiffusive scaling exponent $\nu_1 \approx 0.65$ of the first-order cumulant through spin polarization transfer [Fig. 2(a)] and contrast decay [Fig. 2(c)]. Meanwhile we reconfigure the initial state by adjusting the local spin mixture between S_i^x and S_i^z to reproduce the diffusive transport observed in the SH state. Starting from this modified initial state, i.e., XZ-type MPDW state [Fig. 1(b)], we indeed further observe a diffusive transport emerging with $\nu_1 \approx 0.45$ in the long-time dynamics, see the scaling collapse of contrast decay [Fig. 2(d)] and power-law scaling of relaxation time [inset of Fig. 2(d)]. The consistency of the scaling exponents of the spin polarization transfer and the contrast for different initial states establishes a unified framework for understanding the far-from-equilibrium transport dynamics.

Higher-Order Cumulants via Spin Polarization Transfer

We now turn to main conclusions about higher-order cumulants emerged in far-from-equilibrium transport dynamics. The classical Heisenberg spin chain initiated from an infinite-temperature equilibrium state displays the scaling relation $\nu_{2n} = n\nu_2$ $(n = 1, 2, 3)$ for both superdiffusive $(\nu_2 = 2/3)$ and diffusive $(\nu_2 = 1/2)$ regimes [32]. For the finite-temperature initial states, our analysis of the quantum Heisenberg chain reveals two types of fluctuation dynamics: superdiffusive dynamics with $\nu_{3,4} \approx 2\nu_{1,2}$, and diffusive one with $\nu_{3,4} \approx \nu_{1,2}$. The later is a reminiscence of the chaotic dynamics [42].

Figure 3 illustrates higher-order polarization transfer $|\Delta\mathcal{P}_n(\lambda,t)|$ for the Ising-type MPDW states (a) and for the XZ-type MPDW states (b) in the isotropic Heisenberg spin chain. Here, the gray shaded regions correspond to the analysis domains: $Jt < \lambda/2$ for Ising-type state, and $Jt < \lambda/4$ for XZ-type MPDW state. We clarify that while the scaling of the first three cumulants is stable, the fourth-order cumulant exhibits the expected scaling behavior only within the finite-time window due to quantum fluctuations. The observed instability in the fourth-order cumulant is therefore attributed to genuine long-time quantum fluctuations rather than numerical artifacts. Following same methodology [38–39], guide lines are used to illustrate the scaling behaviors. We observe that the Ising-type initial state (superdiffusive) yields $|\Delta\mathcal{P}_{1,2}(\lambda,t)| \propto t^{0.65}$ and $|\Delta\mathcal{P}_{3,4}(\lambda,t)| \propto t^{1.3}$ [Fig. 3(a)],

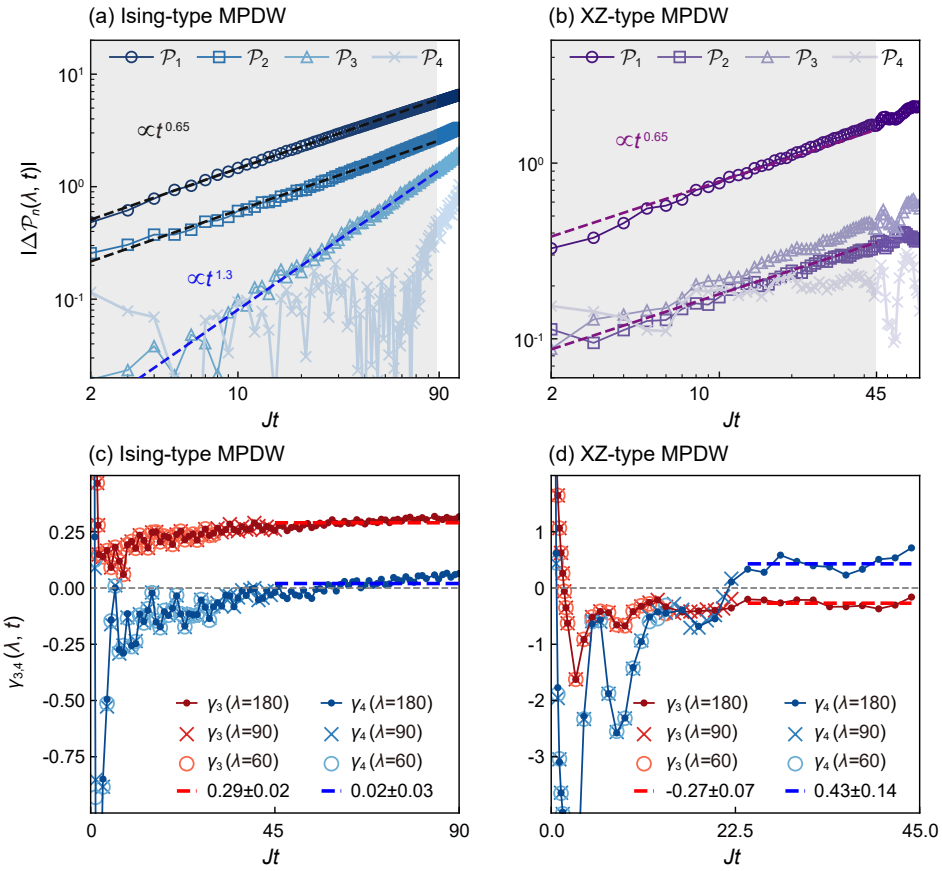

Fig. 3. Higher-order cumulants of spin polarization transfer $|\Delta\mathcal{P}_n(\lambda,t)|$ for Ising-type (superdiffusive) and XZ-type (diffusive) initial states. (a) and (c) For Ising-type MPDW states, (a) third- and fourth-order cumulant exponents ($\nu_3 = 1.24 \pm 0.23$, $\nu_4 = 0.83 \pm 0.59$) are about twice those of the first and second orders ($\nu_1 = 0.65 \pm 0.02$, $\nu_2 = 0.64 \pm 0.05$) with a large system size $L = \lambda = 180$, and (c) standardized cumulants confirm deviation from KPZ universality through skewness $\gamma_3 \approx 0.29 \pm 0.02$ [29] and excess kurtosis $\gamma_4 \approx 0.02 \pm 0.03$ [38]. (b) and (d) For the XZ-type MPDW states, (b) shows approximate scaling exponents with $\nu_1 = 0.45 \pm 0.01$, $\nu_2 = 0.40 \pm 0.03$, $\nu_3 = 0.53 \pm 0.01$, $\nu_4 = 0.20 \pm 0.02$, and (d) non-Gaussian statistics with $\gamma_3 \approx -0.27 \pm 0.07$ and $\gamma_4 \approx 0.43 \pm 0.14$.

reminiscent of previous theoretical predictions for the infinite-temperature Heisenberg model [32]. In contrast to that, the XZ-type initial state (diffusive) demonstrates distinct behavior of the polarization transfer $|\Delta\mathcal{P}_{1,2,3,4}(\lambda,t)| \propto t^{0.45}$, see Fig. 3(b). Our results show that there exist two types of transport belonging to different dynamical universality classes: superdiffusive and diffusive. Here we remark that long-time jitter and divergence in fourth-order cumulant stem from boundary-induced disturbances [38]. Extended finite-size analysis is provided in the SM.

Moreover, we find that deviations from KPZ superdiffusion and normal diffusion are exclusively resolved by the standardized higher-order cumulants. Figures 3(c) and 3(d) show the skewness $\gamma_3(\lambda,t) = \Delta\tilde{\mathcal{P}}_3(\lambda,t)/\Delta\tilde{\mathcal{P}}_2^{3/2}(\lambda,t)$ and excess kurtosis $\gamma_4(\lambda,t) = \Delta\tilde{\mathcal{P}}_4(\lambda,t)/\Delta\tilde{\mathcal{P}}_2^{2}(\lambda,t)$ in the transport dynamics [shaded regions in Figs. 3(a) and 3(b)]. Here, the averaged transfer $\Delta\tilde{\mathcal{P}}_n(\lambda,t) \equiv \Delta\mathcal{P}_n(\lambda,t)/n_c$ with $n_c \equiv 2L/\lambda - 1$ counting the up-down edge points of initial DW structure, e.g., $n_c = 3$ for double-periodic DW state. We find that the Ising-type MPDW states [Fig. 3(c)] result in $\gamma_3 = 0.29 \pm 0.02$ and $\gamma_4 = 0.02 \pm 0.03$ at finite timescales, where these values agree with experimental observations [38] and the latter shows a gradual increasing tendency deviated from the KPZ dynamics [73,74]. Moreover, the XZ-type MPDW states [Fig. 3(d)] give rise to the distinctive non-Gaussian statistics with $\gamma_3 = -0.27 \pm 0.07$ and $\gamma_4 = 0.43 \pm 0.14$, providing anomalous diffusive transport in the integrable quantum system [75]. Note here that the late-stage increase in skewness and excess kurtosis is also a result of finite-size effects, see more detailed analysis in the SM.

In order to further verify the above conclusions, we employ FCS to characterize spin transport fluctuations. This method extracts the cumulants from the quantum generating function of the spin polarization transfer [2,34,39]. The detailed formulas and dynamical scalings for Ising- and XZ-type MPDW states are given in the SM. In addition, quantum fluctuations versus subsystem sizes [33] provides an alternative tool for extracting scaling exponents of the higher-order cumulants, and more discussions are given in the SM.

Higher-Order Cumulants from Contrast

To further examine transport behavior in higher-order cumulants, we extract scaling exponents from the contrast $\mathcal{K}_n(\lambda,t)$ in the far-from-equilibrium dynamics of the Heisenberg chain. For both XZ-type MPDW and SH initial states, time evolution generates spatial correlations between sites, producing finite higher-order cumulants. Figure 4(a) shows the third-order contrast $\mathcal{K}_3$ for the SH initial state, where we observe that it rises to a maximum at time τ before decaying. As expected, the third-order cumulant exhibits scaling collapse when rescaled by λ^{1/ν_3}, see inset of Fig. 4(a). The scaling exponent ν_3 is identical to the prediction from the first-order contrast decay with $\nu_1 = \nu_3$ [Fig. 2(b)]. A discussion on the rescaled dynamics of $\mathcal{K}_{2,4}$ is provided in the SM.

In addition, the growth threshold time τ for the contrast $\mathcal{K}_{2,3,4}$ reaching their respective first maxima also exhibits power-law scaling $\tau \propto \lambda^{1/\nu_n}$. In Figs. 4(b) and 4(c), we plot the threshold time τ versus wavelength λ for the SH (b) and the XZ-type MPDW states (c), confirming that the scaling of cumulant dynamics exhibit identical exponents $\nu_{1,2,3,4} \approx 0.45$ for both SH and XZ-type MPDW states. The consistency with the scaling exponents obtained from spin polarization transfer measurement $|\Delta\mathcal{P}_n|$ [Fig. 3(b)] and contrast analysis $\mathcal{K}_n$ [Figs. 4(b) and 4(c)] validates the reliability of characteristic of the higher-order cumulants in the far-from-equilibrium dynamics.

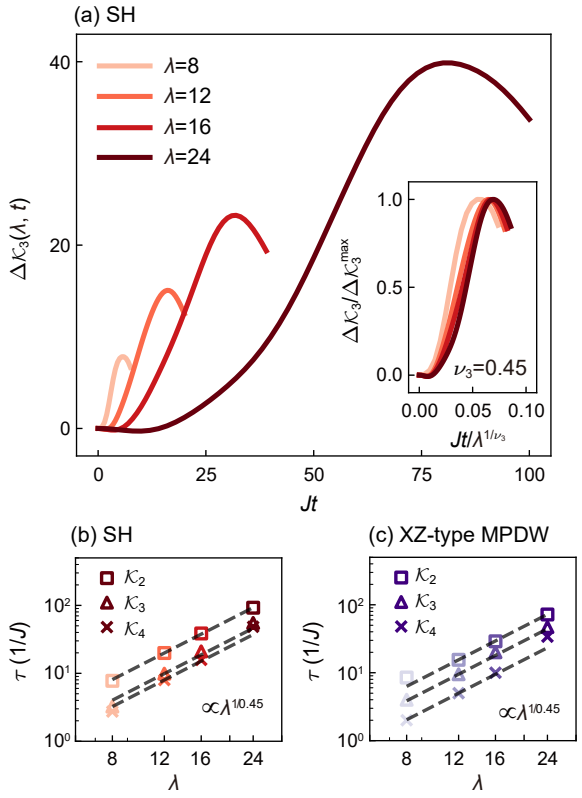

Fig. 4. Higher-order cumulants via contrast $\mathcal{K}_n(\lambda,t)$ for XZ-type MPDW (diffusive) and SH (diffusive) initial states. (a) shows contrast dynamics of the third-order cumulant $\mathcal{K}_3(\lambda,t)$ for the SH states with different wavelengths. The inset shows data collapse of rescaled contrast from (a), where $\Delta\mathcal{K}_3 \equiv \mathcal{K}_3(\lambda,t)-\mathcal{K}_3(\lambda,0)$ and $\Delta\mathcal{K}_3^{\max}$ denotes the first maximum. (b) and (c) Power-law scaling of the growth threshold time τ when the cumulant reaches its first maximum, versus wavelength λ for the second- (□), third- (△) and fourth-order (×) cumulants for different initial states: (b) SH and (c) XZ-type MPDW states, respectively. Scaling exponents from contrast agree with those obtained via spin polarization transfer. Specifically, SH state shows $\nu_2 = 0.50\pm0.01$, $\nu_3 = 0.40\pm0.01$ and $\nu_4 = 0.39\pm0.01$. XZ-type MPDW state shows $\nu_2 = 0.50\pm0.02$, $\nu_3 = 0.45\pm0.01$ and $\nu_4 = 0.39\pm0.01$. Details see in the SM. Lattice size is $L = 96$.

Summary and Outlook

We have developed a theoretical framework to capture the higher-order universal scaling of far-from-equilibrium transport dynamics in the 1D quantum Heisenberg model. Using numerical simulations and full counting statistics, we have rigorously computed scaling laws for higher-order cumulants of previously uncharacterized spin-helix (SH) and domain-wall (DW) initial states. This scaling behavior, specifically for spin polarization transfer and contrast cumulants of experimentally accessible initial states, is categorized into two dynamical regimes: anomalous diffusion and superdiffusion. For the former, the first four cumulants share identical scaling exponents; for the latter, the exponents of the third and fourth cumulants differ markedly from those of the first two. Our findings are consistent with recent experiments [34,35,38], and further highlight the critical role of higher-order nonlocal correlations in unraveling far-from-equilibrium transport dynamics across diverse systems, including ultracold atoms and superconducting compounds [34,35,38]. From our numerical results, the higher-order cumulant scaling laws become visible at $Jt \gtrsim 10$, suggesting that this dynamical scaling is accessible in the current cold-atom experiments [34–37]. These anomalous dynamical behaviors resolve the long-standing open question of whether higher-order cumulants obey universal scaling laws in diffusive and superdiffusive regimes when approaching asymptotic diffusion [49–52]. Moreover, our approach can be extended to investigate long-time dynamics in low-dimensional doped strongly correlated fermionic systems, probing how higher-order cumulants encapsulate the core features of spin-charge separation [76,77].

Acknowledgments

We acknowledge useful discussions with Angelo Valli, Zhensheng Yuan, Lei Feng, and Xuchen Yang. Y.L. acknowledges the support by the National Natural Science Foundation of China (Grant Nos. 12074431, 12374252, and 12274384), and the Science and Technology Innovation Program of Hunan Province (Grant No. 2024RC1046). J.L. acknowledges the support by the National Natural Science Foundation of China (Grant No. 12404332). X.W.G. is supported by the NSFC key (Grant No. 12134015), the NSFC key (Grant No. 92365202), and the Innovation Program for Quantum Science and Technology (Grant No. 2021ZD0302000).

References

[1] Landi G T, Poletti D, and Schaller G 2022 *Rev. Mod. Phys.* **94** 045006
[2] Esposito M, Harbola U, and Mukamel S 2009 *Rev. Mod. Phys.* **81** 1665
[3] Polkovnikov A, Sengupta K, Silva A, and Vengalattore M 2011 *Rev. Mod. Phys.* **83** 863
[4] Bertini B, Heidrich-Meisner F, Karrasch C, Prosen T, Steinigeweg R, and Žnidarič M 2021 *Rev. Mod. Phys.* **93** 025003
[5] Guan X W and He P 2022 *Rep. Prog. Phys.* **85** 114001
[6] He W B and Guan X W 2018 *Chin. Phys. Lett.* **35** 110302
[7] Wyatt R E 2005 *Quantum Dynamics with Trajectories: Introduction to Quantum Hydrodynamics* (Springer New York, NY)
[8] Bulchandani V B, Gopalakrishnan S, and Ilievski E 2021 *J. Stat. Mech.* **2021** 084001
[9] Ye B, Machado F, Kemp J, Hutson R B, and Yao N Y 2022 *Phys. Rev. Lett.* **129** 230602
[10] Ilievski E, De Nardis J, Medenjak M, and Prosen T 2018 *Phys. Rev. Lett.* **121** 230602
[11] Gopalakrishnan S and Vasseur R 2019 *Phys. Rev. Lett.* **122** 127202
[12] De Nardis J, Medenjak M, Karrasch C, and Ilievski E 2019 *Phys. Rev. Lett.* **123** 186601
[13] Scheie A, Sherman N, Dupont M, Nagler S, Stone M, Granroth G, Moore J, and Tennant D 2021 *Nat. Phys.* **17** 726
[14] Žnidarič M 2011 *Phys. Rev. Lett.* **106** 220601
[15] Gopalakrishnan S, Vasseur R, and Ware B 2019 *Proc. Nat. Acad. Sci.* **116** 16250
[16] Gopalakrishnan S and Vasseur R 2023 *Rep. Prog. Phys.* **86** 036502
[17] Ljubotina M, Žnidarič M, and Prosen T 2019 *Phys. Rev. Lett.* **122** 210602
[18] Yu Y C and Guan X W 2017 *Chin. Phys. Lett.* **34** 070501
[19] Kardar M, Parisi G, and Zhang Y C 1986 *Phys. Rev. Lett.* **56** 889
[20] Popkov V, Schadschneider A, Schmidt J, and Schütz G M 2015 *Proc. Nat. Acad. Sci.* **112** 12645
[21] De Nardis J, Doyon B, Medenjak M, and Panfil M 2022 *J. Stat. Mech.* **2022** 014002
[22] Ljubotina M, Zadnik L, and Prosen T 2019 *Phys. Rev. Lett.* **122** 150605
[23] Feldmeier J, Sala P, De Tomasi G, Pollmann F, and Knap M 2020 *Phys. Rev. Lett.* **125** 245303
[24] Ljubotina M, Desaules J Y, Serbyn M, and Papić Z 2023 *Phys. Rev. X* **13** 011033
[25] Cecile G, De Nardis J, and Ilievski E 2024 *Phys. Rev. Lett.* **132** 130401
[26] Georgescu I M, Ashhab S, and Nori F 2014 *Rev. Mod. Phys.* **86** 153
[27] Hübner F, Biagetti L, De Nardis J, and Doyon B 2025 *Phys. Rev. Lett.* **134** 187101
[28] Joshi M K, Kranzl F, Schuckert A, Lovas I, Maier C, Blatt R, Knap M, and Roos C F 2022 *Science* **376** 720
[29] Prähofer M and Spohn H 2000 *Phys. Rev. Lett.* **84** 4882
[30] Doyon B, Perfetto G, Sasamoto T, and Yoshimura T 2023 *SciPost Phys.* **15** 136
[31] Myers J, Bhaseen M J, Harris R J, and Doyon B 2020 *SciPost Phys.* **8** 007
[32] Krajnik Ž, Schmidt J, Ilievski E, and Prosen T 2024 *Phys. Rev. Lett.* **132** 017101
[33] Wienand J F, Karch S, Impertro A, Schweizer C, McCulloch E, Vasseur R, Gopalakrishnan S, Aidelsburger M, and Bloch I 2024 *Nat. Phys.* **20**

1732
[34] Wei D, Rubio-Abadal A, Ye B, Machado F, Kemp J, Srakaew K, Hollerith S, Rui J, Gopalakrishnan S, Yao N Y, Bloch I, and Zeiher J 2022 *Science* **376** 716
[35] Jepsen P N, Amato-Grill J, Dimitrova I, Ho W W, Demler E, and Ketterle W 2020 *Nature* **588** 403
[36] Jepsen P N, Ho W W, Amato-Grill J, Dimitrova I, Demler E, and Ketterle W 2021 *Phys. Rev. X* **11** 041054
[37] Jepsen P N, Lee Y K E, Lin H, Dimitrova I, Margalit Y, Ho W W, and Ketterle W 2022 *Nat. Phys.* **18** 899
[38] Rosenberg E, Andersen T, Samajdar R *et al* 2024 *Science* **384** 48
[39] Valli A, Moca C P, Werner M A, Kormos M, Krajnik Ž, Prosen T, and Zaránd G 2025 *Phys. Rev. Lett.* **135** 100401
[40] Takeuchi K A, Takasan K, Busani O, Ferrari P L, Vasseur R, and De Nardis J 2025 *Phys. Rev. Lett.* **134** 097104
[41] De Nardis J, Gopalakrishnan S, and Vasseur R 2023 *Phys. Rev. Lett.* **131** 197102
[42] McCulloch E, De Nardis J, Gopalakrishnan S, and Vasseur R 2023 *Phys. Rev. Lett.* **131** 210402
[43] Bertini B, Calabrese P, Collura M, Klobas K, and Rylands C 2023 *Phys. Rev. Lett.* **131** 140401
[44] Samajdar R, McCulloch E, Khemani V, Vasseur R, and Gopalakrishnan S 2024 *Phys. Rev. Lett.* **133** 240403
[45] Krajnik Ž, Schmidt J, Pasquier V, Ilievski E, and Prosen T 2022 *Phys. Rev. Lett.* **128** 160601
[46] Krajnik Ž, Ilievski E, and Prosen T 2022 *Phys. Rev. Lett.* **128** 090604
[47] Mao L, Zhai H, and Yang F 2025 *Chin. Phys. Lett.* **42** 067401
[48] Ljubotina M, Žnidarič M, and Prosen T 2017 *Nat. Commun.* **8** 16117
[49] Misguich G, Mallick K, and Krapivsky P L 2017 *Phys. Rev. B* **96** 195151
[50] Ljubotina M, Žnidarič M, and Prosen T 2017 *J. Phys. A: Math. Theo.* **50** 475002
[51] Misguich G, Pavloff N, and Pasquier V 2019 *SciPost Physics* **7** 025
[52] Gamayun O, Miao Y, and Ilievski E 2019 *Phys. Rev. B* **99** 140301
[53] Hild S, Fukuhara T, Schauß P, Zeiher J, Knap M, Demler E, Bloch I, and Gross C 2014 *Phys. Rev. Lett.* **113** 147205
[54] Popkov V, Zhang X, Göhmann F, and Klümper A 2024 *Phys. Rev. Lett.* **132** 220404
[55] Smith P J 1995 *Am. Stat.* **49** 217
[56] Holtermann A, Noronha-Hostler J, Sickles A M, and Wang X 2023 *Phys. Rev. C* **108** 064901
[57] Royer A 1972 *Phys. Rev. A* **6** 1741
[58] Parrinello M and Arai T 1974 *Phys. Rev. B* **10** 265
[59] Hirayama R, Grassi F, Serenone W M, and Ollitrault J Y 2023 *Phys. Rev. C* **107** 024910
[60] Fishman M, White S R, and Stoudenmire E M 2022 *SciPost Phys. Codebases* 4
[61] Haegeman J, Cirac J I, Osborne T J, Pižorn I, Verschelde H, and Verstraete F 2011 *Phys. Rev. Lett.* **107** 070601
[62] Goto S and Danshita I 2019 *Phys. Rev. B* **99** 054307
[63] Gleis A, Li J W, and von Delft J 2023 *Phys. Rev. Lett.* **130** 246402
[64] Yang M and White S R 2020 *Phys. Rev. B* **102** 094315
[65] Popkov V, Zhang X, and Klümper A 2021 *Phys. Rev. B* **10** 4
[66] Pereira D and Mueller E J 2022 *Phys. Rev. A* **106** 043306
[67] Pereira D and Mueller E J 2024 *Phys. Rev. A* **110** 023313
[68] Popkov V, Žnidarič M, and Zhang X 2023 *Phys. Rev. B* **107** 235408
[69] Cecile G, Gopalakrishnan S, Vasseur R, and De Nardis J 2023 *Phys. Rev. B* **108** 075135
[70] Zhang X, Klümper A, and Popkov V 2021 *Phys. Rev. B* **103** 115435
[71] Zhang X, Klümper A, and Popkov V 2021 *Phys. Rev. B* **104** 195409
[72] Kühn S, Gerken F, Funcke L, Hartung T, Stornati P, Jansen K, and Posske T 2023 *Phys. Rev. B* **107** 214422
[73] Baik J and Rains E M 2000 *Journal of Statistical Physics* **100** 523
[74] Tracy C A and Widom H 1994 *Commun. Math. Phys.* **159** 151
[75] Gopalakrishnan S, Morningstar A, Vasseur R, and Khemani V 2024 *Phys. Rev. B* **109** 024417
[76] Giamarchi T 2003 *Quantum Physics in One Dimension* (Oxford University Press)
[77] Senaratne R, Cavazos-Cavazos D, Wang S, He F, Chang Y T, Kafle A, Pu H, Guan X W, and Hulet R G 2022 *Science* **376** 1305